Conformational Characteristics of Poly(D-β-hydroxybutyrate)

Robert E. Kyles† and Alan E. Tonelli*

North Carolina State University, Fiber & Polymer Science, Campus Box 8301, Raleigh, North Carolina 27695-8301

Received January 17, 2002; Revised Manuscript Received November 29, 2002

ABSTRACT: We present characteristic ratios of the unperturbed dimensions $C_r = \langle r^2\rangle_o/n\langle l^2\rangle$, where $\langle r^2\rangle_o$ is the mean-square unperturbed end-to-end distance and n is the number and $\langle l^2\rangle$ is the mean-square length of the backbone bonds, calculated for poly(D-β-hydroxybutyrate) (PHB) chains with traditional rotational isomeric state (RIS) models, a computer-generated RIS model, and molecular dynamics simulations of isolated PHB chains. These dimensions are compared with those reported in the literature for PHB observed in both dilute solutions ($C_r \sim 8$) and in the bulk melt ($C_r \sim 40$). The traditional and computer-generated RIS models yield $C_r \sim 3-4$, while $C_r \sim 8$ is obtained from the molecular dynamics simulation of isolated PHB chains. In addition we find that the dimensions calculated for PHB chains are independent of their stereosequence. A search for the occurrence and correlation of PHB repeat units adopting the crystalline helical conformation conducted during the molecular dynamics simulation failed to uncover the source for the unusually large dimensions ($C_r \sim 40$) reported for PHB chains in the amorphous bulk. We do observe, however, that the conformations of PHB repeat units are not totally independent of the conformations of neighboring repeat units, as would normally be expected for polyesters with rigid trans ester bonds. Nevertheless, we find PHB to be a conformationally diverse and flexible, randomly coiling polymer with dimensions not atypical for aliphatic polyesters, consistent with the behavior observed for PHB in dilute solution but not by SANS in the amorphous bulk.

Introduction

The aliphatic polyester poly(D-β-hydroxybutyrate) (PHB) illustrated in Figure 1 was first isolated from bacteria,[1] where it functions as a stored energy reserve.[2−5] PHB has glass-transition and melting temperatures[6] close to those of the synthetic thermoplastic polypropylene (PP) and was originally sought as a biodegradable/bioabsorbable replacement for PP. However, PHB is thermally unstable at processing temperatures and too brittle for industrial applications, and so biosynthetically produced copolymers of β-HB and β-hydroxyvalerate were developed[7] to remedy these shortcomings and have achieved limited commercial applications.

PHB crystallizes into a left-handed 2_1-helix with an approximately g^+g^+tt conformation[8,9] as drawn in Figure 2. On the basis of their optical rotatory dispersion (ORD) observations, Marchessault et al.[10] proposed that PHB can either randomly coil or be at least partially helical in solution depending on the solvent and temperature. Coupled with accompanying light-scattering observations,[11] they were led to suggest that PHB chains may adopt folded helical conformations in solution leading to ellipsoidal, rigid rodlike particles composed of the folded PHB helices.

Einaga et al.[12,13] subsequently observed the dilute solution properties of a series of fractionated PHBs covering a wide range of molecular weights.

They were unable to reproduce the ORD observations of Marchessault et al.,[10] which had suggested a propensity for PHB helices in some solutions. In addition, they reported extensive light-scattering and viscosity observations which led to the conclusion that, though highly expanded by excluded volume self-intersections in certain good solvents like trifluoroethylene, PHB chains are essentially randomly coiling in solution. When their data are extrapolated[14] to unperturbed conditions, the resulting dimensions $C_r \sim 8$ are obtained. Subsequently

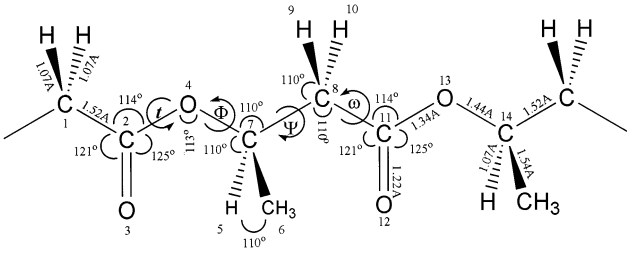

Figure 1. Schematic drawing of PHB showing structural parameters adopted[18] for the conformational energy calculations used to develop the RIS model.

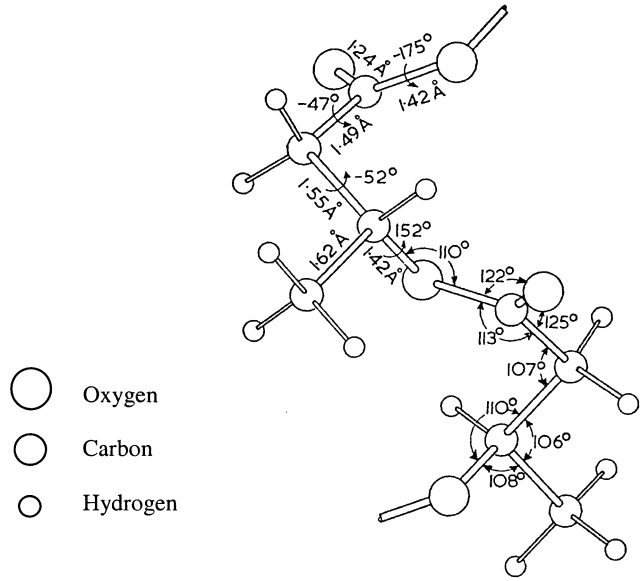

Figure 2. Drawing of a molecular model of PHB in its crystalline[8,9] conformation.

† Currently with Lord Corporation, Cary, NC.

10.1021/ma0200827 CCC: $25.00
Published on Web 01/25/2003

Huglin and Radwan[15] have observed PHBs in mixed Θ solvents and have reported unperturbed dimensions ($C_r \sim 8$) very close to those extrapolated from the data of Einaga et al.

Doi et al.[16] have most recently reported on deuterated PHB (d-PHB) that was produced biosynthetically and melt blended with a fully protonated, synthetic atactic poly(D,L-β-hydroxybutyrate) (a-PHB) and then quenched into a sample (5/95 d-PHB/a-PHB) that was examined by small-angle neutron scattering (SANS). From the angular dependence of the scattered neutron intensity, they obtained the persistence length of the d-PHB, which they said reflected "a high degree of local chain persistence". The unperturbed dimensions obtained from their persistence length was $C_r \sim 40$. Though the d-PHB chain was found on average to be highly persistent locally, globally the PHB chains appeared to be Gaussian as judged by the scattered neutron intensities observed at low angles. They also report similar large unperturbed dimensions ($C_r \sim 40$) for PHB obtained from viscometry measurements cited as "in preparation" but that, to our knowledge, were never subsequently published.

Here we describe an attempt to characterize the conformational characteristics of PHB chains using traditional and computer-generated RIS conformational models and molecular dynamics simulations of isolated PHB chains. In addition, through an analysis of the conformations of contiguous PHB repeat units observed during the molecular dynamics trajectories and by fixing contiguous PHB repeat units in extended helical conformations when calculating average dimensions for PHB chains with the RIS models, we probe the propensity for unperturbed PHB chain contours to persist locally in an effort to understand the conformational origin of the large dimensions ($C_r \sim 40$) reported[16] for bulk amorphous d-PHB chains from SANS measurements.

Description of the Conformational Calculations

1. Traditional RIS Model. A traditional RIS model, as outlined by Flory,[17] was constructed for PHB using the geometric and energetic parameters employed by Brant et al.[18] to treat a similar aliphatic polyester poly(L-lactic acid). The energies corresponding to the three rotational bond pairs (τ,ϕ); (ϕ,ψ); (ψ,ω) in each PHB repeat unit (see Figure 1) were calculated in 10° increments for each rotation angle of the pair, and only the interactions between atoms and/or groups whose distances of separation depend on either or both of the pairs of rotation angles were considered. In addition, the energy of the entire PHB repeat unit, E_{conf}, was calculated, and of course this repeat unit energy depends simultaneously on all four backbone torsions τ, φ, ψ, and ω. Because the ester bond possesses partial double bond character, we maintained it in the planar trans conformation t, with $\tau = 0°$.

Statistical weights $\mu_{\alpha\beta,i}$, for each rotational state α of bond $i-1$ and β of bond i, were calculated from the normalized conformational energies $E_{\alpha\beta,i}$ as $\mu_{\alpha\beta,i} = \exp[-E_{\alpha\beta,i}/RT]$. When constructing the statistical weight matrices, $\mathbf{U}_i$, for each backbone bond, the bond-pair statistical weights were summed over the discrete rotational states as given by trans = t = 310−60°, gauche$^+$ = g$^+$ = 70−180°, and gauche$^-$ = g$^-$ = 190−300°. Statistical weight matrices for each of the three bond pairs of the PHB repeat unit (see Figure 1) were also calculated from the total repeat unit energy E_{conf} by the same procedure, except each constituent bond-pair statistical weight $\mu_{\alpha\beta,i}$ was evaluated by summing all values of E_{conf} over the full ranges of the remaining two rotation angles in the repeat unit. For example, if $\alpha\beta = \varphi\psi$, then for each bond-pair conformation $\varphi\psi$, we summed over all E_{conf} values corresponding to the full ranges of τ and ω backbone rotations.

With these statistical weight matrices and using the matrix multiplication methods described by Flory,[17] we calculated the unperturbed mean-square end-to-end distances $\langle r^2\rangle_o$ of PHB chains. $\langle l^2\rangle = 2.117$ Å^2, so $C_r = \langle r^2\rangle_o/4N\langle l^2\rangle = \langle r^2\rangle_o/(8.468N)$, where $N = n/4$ is the number of repeat units in the PHB chain.

2. Computer-Generated RIS Model. A computer-generated RIS model for PHB was developed with the Biosym/MSI (San Diego, CA) molecular modeling package, release 3.0.0. The *Insight II* user interface was used to run the *RIS* module within the *Polymer 3.0.0* software package. This software utilizes the *Discover* program to perform conformational energy calculations with the CVFF force field. The modeling was performed on a Silicon Graphics Indigo-2 Impact 10000 workstation. Because none of the backbone bond-pairs in PHB were found in the *RIS* module properties library, each bond-pair ($\tau\varphi$, $\varphi\psi$, $\psi\omega$, $\omega\tau$) was incorporated into a separate appropriate small molecule, and the *Discover* program was used to calculate the conformational energies at 10° increments for each of the constituent bond-pair rotation angles. The same dielectric constant $\epsilon = 3$ was used[18] as in the traditional RIS analysis, and the conjugate gradient minimization algorithm was employed. All bond lengths and valence angles were determined by the software package.

Statistical weight matrices for each bond-pair were determined from the appropriate small molecule conformational energy maps by the software package, which locates energy minima, averages the angles in the region about each energy minimum, and calculates the statistical weight of each low energy region. With these computer-generated locations and statistical weights for each bond-pair conformation and the associated geometries, a calculation of the characteristic ratio of the dimensions C_r was performed as a function of PHB chain length.

3. Molecular Dynamics Simulation of PHB. (a) Amorphous Cell Simulation. Initially we attempted to perform a molecular dynamics simulation of an amorphous cell of PHB under periodic boundary conditions,[19] using the *Amorphous_Cell* module and a 10 repeat unit PHB chain (10-mer) in a 10.52 Å cube, which corresponds to the observed amorphous density of 1.23 g/cm^3 for PHB.[6] The initially packed PHB cell was refined to remove molecular overlaps and other high energy structures by running 100 000 1-fs steps of canonical (*NVT*) dynamics. Velocity scaling maintained a constant temperature, and the energy expressions (CVFF) were integrated with the Verlet velocity algorithm. After this refinement, the dynamics simulation was started with 1000 steps of minimization followed by up to 12 ns of dynamics, during which data were collected. However, even at a temperature of 500 K, the 10 repeat unit PHB chain did not sample a significant portion of its conformational space as indicated in Figures 3 and 4.

End-to-end distances observed for the PHB 10-mer during its 12 ns amorphous cell dynamics simulation

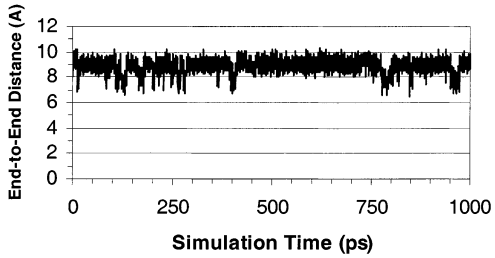

Figure 3. End-to-end distances of the PHB 10-mer observed during its amorphous cell molecular dynamics simulation.

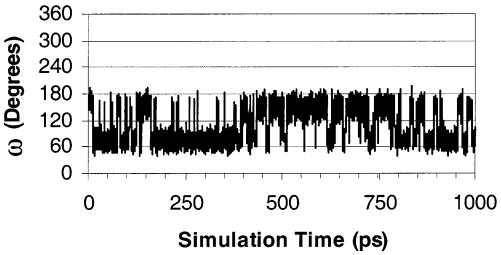

Figure 4. Variation of the ω internal rotation angle during the amorphous cell dynamics simulation of a PHB 10-mer conducted at 298 K.

are presented in Figure 3, where it is clear that only a few significant conformational changes have taken place during the course of this lengthy dynamics trajectory. This conclusion is reinforced by the plots of the ø, ψ, and ω backbone torsions observed in an internal repeat unit of the PHB 10-mer over the course of the dynamics trajectory (see Figure 4, for example). Examination of these plots reveals a preponderance of torsional oscillations within rotational states, but very infrequent transitions between rotational states, which are necessary for a full sampling of PHB conformations and subsequent calculation of its overall average dimensions. As a consequence, we abandoned the amorphous cell dynamics simulation of PHB and turned instead to the examination of the dynamics of isolated PHB chains.

(b) Isolated Chain Simulation. Following a recent study by Hedenqvist et al.,[20] we chose to model unconfined and isolated PHB chains. The conformational characteristics of PET were investigated by these workers through a molecular dynamics simulation of single unconfined and isolated chains, termed a "phantom chain"[21] dynamics simulation. Their simulation reproduced the observed unperturbed dimensions of PET. Like the RIS treatment of polymer conformations, the phantom chain simulation is governed exclusively by the intramolecular energetic interactions, but in the phantom chain simulation these may be longer in range, i.e., between atoms further removed along the chain contour. When the conformation of the polymer chain places segments within a specified through-space cutoff distance, regardless of their separation along the chain contour, their interaction is included in the energetic calculation, giving rise to an accounting of excluded volume effects.

The phantom chain calculations performed on unconfined and isolated PHB chains were performed using the *Discover_3* module of the Biosym/MSI (San Diego, CA) software package. Again $\epsilon = 3$ was selected and electrostatic and van der Waals potentials were set to cutoff at a finite distance. Following Hedenqvist et al., we set the cutoff distance to approximate the length of one PHB repeat unit in the all trans conformation, which is 4.85 Å, and so we employed a cutoff distance

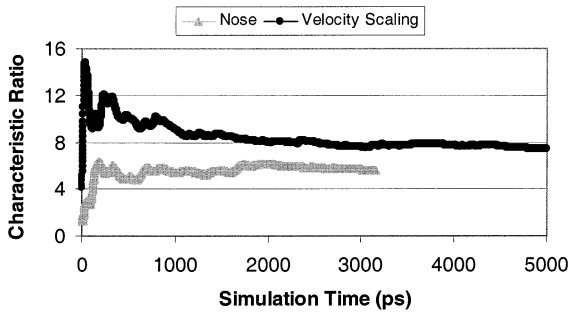

Figure 5. Characteristic ratios, C_r, calculated for a PHB 60-mer chain using velocity scaling and the Nose method of temperature control during the phantom chain dynamics simulations.

of 5.0 Å in our simulations. PHB chains of 10, 60, 100, and 200 repeat units were simulated. The 10 repeat unit chain (10-mer) was conditioned with 5000 steps of initial energy minimization and equilibrated with 1 ns of dynamics with 1-fs time steps, followed by a 2 ns dynamics run with data sampling every 50 fs. The 60, 100, and 200 repeat unit PHB chains (60-, 100-, and 200-mers) were conditioned with 5000 steps of initial minimization, followed by 100 000 fs steps of dynamics, and then re-minimized for 5000 steps and equilibrated with 1 ns of dynamics. Following this preparation, a 5 ns dynamic run was conducted with 1-fs time steps and data sampling every 1 ps. All phantom chain dynamics simulation were run at 298 K under *NVT* constraints and employed the CVFF force field.

In addition, the 60-mer phantom chain dynamics simulation was repeated, but instead of beginning from a randomly generated chain conformation, the PHB chain was initially placed in the crystalline 2_1-helical conformation ($\tau = 0°$, $\varphi = 332°$, $\psi = 128°$, $\omega = 133°$; see Figure 2), and then the molecular dynamics simulation was conducted identically. A Fortran 77 program was written to search the PHB 60-mer molecular dynamics trajectory for the occurrence and persistence of repeat units adopting the helical conformation. This program sequentially reads the conformations of each of the 20 internal repeat units (repeat units 21−40) and determines whether the values of each repeat unit torsion angle falls within ±30° of the helical value. A count was made of both the total number of helical repeat units and the numbers of successive helical repeat units.

The default force field CVFF used by all Biosym/MSI (San Diego, CA) software modules yielded a RIS model for PHB that was very similar to that obtained with the Brant et al.[18] force field. Also, a short simulation of the PHB 60-mer, employing the Nosé-Hoover method of temperature control,[23−26] was conducted and compared to the velocity scaling method, resulting in similar characteristic dimensions as shown in Figure 5. Therefore, we chose to utilize the CVFF force field and the velocity scaling method of temperature control in all of the molecular dynamics simulations reported here.

Results and Discussion

1. PHB RIS Models and Dimensions. (a) Traditional RIS Model. Figures 6−8 present the results of the conformational energy calculations used to construct the statistical weight matrices for the traditional RIS model, which are necessary for evaluation of the unperturbed dimensions of PHB and are shown below. In

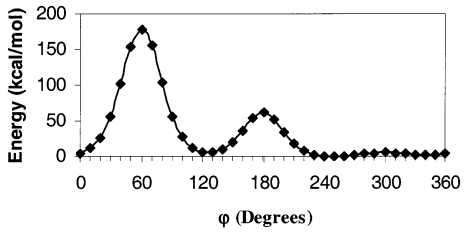

Figure 6. Energy curve for the PHB backbone φ torsion used to develop the traditional RIS model, where energies are in kcal/mol.

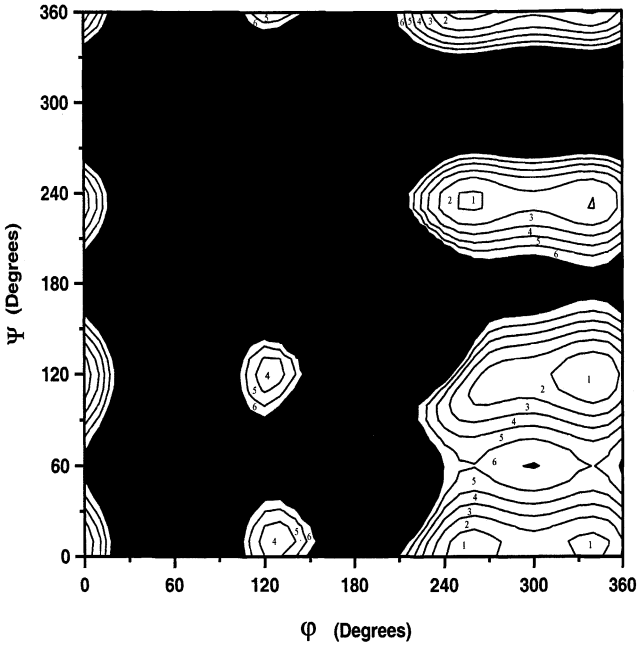

Figure 7. RIS energy map for the φ,ψ pair of PHB backbone torsions, where the energy contours $E(\varphi,\psi)$ are given in kcal/mol.

addition, the statistical weight matrices

$$\mathbf{U}_{\phi} = \begin{bmatrix} 5.94\text{E}{-}02 & 4.29\text{E}{-}05 & 0.940513 \\ 0 & 0 & 0 \\ 0 & 0 & 0 \end{bmatrix}$$

$$\mathbf{U}_{\phi\psi} = \begin{bmatrix} 0.137003 & 0.393369 & 8.18\text{E}{-}02 \\ 9.04\text{E}{-}04 & 7.10\text{E}{-}04 & 3.07\text{E}{-}08 \\ 0.219524 & 5.93\text{E}{-}02 & 0.107397 \end{bmatrix}$$

$$\mathbf{U}_{\psi\omega} = \begin{bmatrix} 1.88\text{E}{-}02 & 2.81\text{E}{-}02 & 7.51\text{E}{-}02 \\ 0.12272 & 0.375973 & 0.332988 \\ 1.90\text{E}{-}03 & 298\text{E}{-}02 & 1.46\text{E}{-}02 \end{bmatrix}$$

constructed from the full PHB repeat unit conformational energies E_{conf} are also presented.

$$\mathbf{U}_{\phi} = \begin{bmatrix} 0.444551 & 0 & 0.555449 \\ 0 & 0 & 0 \\ 0 & 0 & 0 \end{bmatrix}$$

$$\mathbf{U}_{\phi\psi} = \begin{bmatrix} 3.51\text{E}{-}02 & 0.391801 & 1.76\text{E}{-}02 \\ 0 & 0 & 0 \\ 0.284856 & 5.40\text{E}{-}02 & 0.216631 \end{bmatrix}$$

$$\mathbf{U}_{\psi\omega} = \begin{bmatrix} 4.26\text{E}{-}02 & 5.78\text{E}{-}02 & 0.219583 \\ 8.10\text{E}{-}02 & 0.241148 & 0.123655 \\ 1.51\text{E}{-}02 & 0.109401 & 0.10972 \end{bmatrix}$$

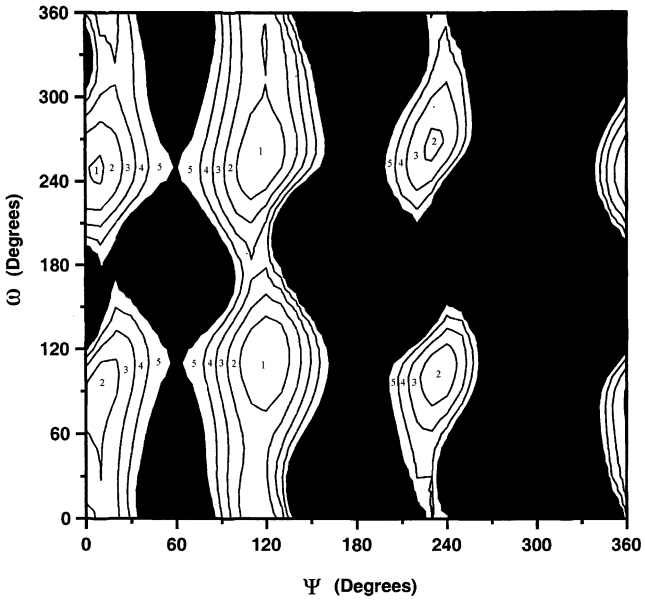

Figure 8. Same as Figure 6, except replace φ,ψ with ψ,ω

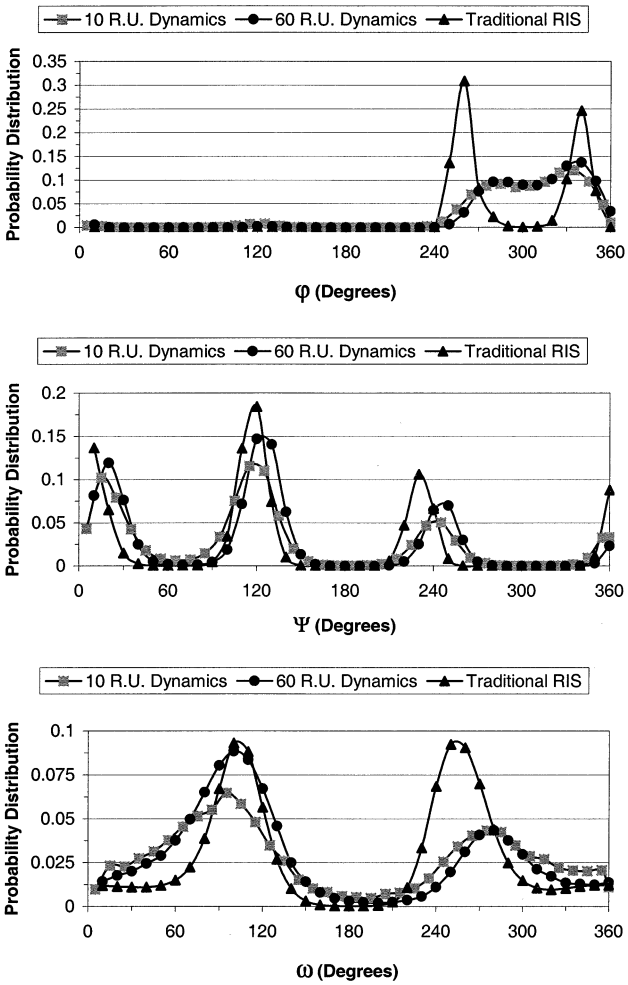

Figure 9. Comparison of the probability distributions for PHB backbone rotations obtained from the traditional RIS model and the phantom chain dynamics simulations of the PHB 10- and 60-mers.

The probabilities for each backbone torsion in the PHB repeat unit obtained from the conformational energies of Figures 6−8 are given in Figure 9. The φ torsion adopts only the g^- and t conformations, with each shifted ±20° toward each other. The ψ torsion is

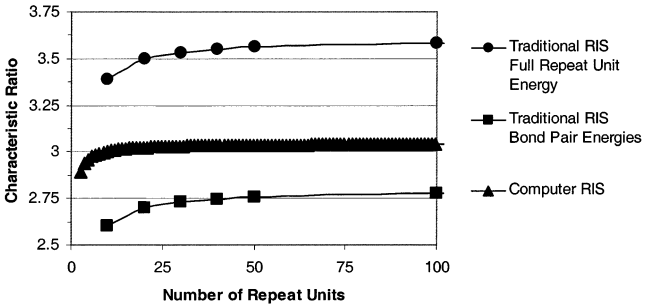

Figure 10. Characteristic ratios, C_r, calculated for PHB chains of varying lengths n using the traditional RIS models and the computer-generated RIS model.

more closely aligned with the three traditional RIS states (0, 120, 240°), with a slight preference for the g^+ conformation. The ω torsion shows high, almost equal probabilities for the two gauche conformers, which are displaced $\sim\pm20°$ from the traditional g^- and g^+ RIS states. In addition, there is no maximum for the t state, but a finite probability is maintained as ω is rotated from $g^+ \rightarrow t \rightarrow g^-$, implying a low energy barrier for this conformational transition.

The dimensions $C_r = \langle r^2\rangle_o/n\langle l^2\rangle$ calculated for PHB chains as a function of chain length $N = n/4$ from the traditional and modified RIS models are shown in Figure 10. C_r is seen to increase with chain length and rapidly plateau to values of C_r ($n \rightarrow \infty = C_\infty$) = 2.8 and 3.6 when calculated from the traditional RIS models derived from individual bond-pair and full repeat unit conformational energies, respectively. The additional constraint placed on the PHB backbone torsions by considering energetic interactions of longer range, i.e., between atoms and/or groups separated by six vs four bonds, apparently results in an ~30% increase in the average $\langle r^2\rangle_o$ calculated for PHB. It should also be mentioned that these calculated dimensions were found to be independent of PHB repeat unit stereochemistry. Isotactic, syndiotactic, and atactic PHBs, having all D or all L, alternating D and L, and 50% D, 50% L randomly placed repeat units, respectively, have the same calculated C_rs. Stereosequence-independent dimensions argue strongly against a propensity for PHB chains to adopt local helical conformations spanning several repeat units.

(b) Computer-Generated RIS Model. In Figure 10, the dimensions calculated for PHB chains from the computer-generated RIS model are shown to increase with chain length as rapidly as those obtained from the traditional RIS models and to plateau at $C_\infty = 3.04$, which lies between the traditional values.

(c) Molecular Dynamics Simulation. (1) PHB 10-mer. The end-to-end distances of the PHB 10-mer during its molecular dynamics simulation are presented in Figure 11, where it can be clearly seen that the 10-mer has randomly sampled virtually all of its conformational space, because end-to-end distances nearly covering the complete range from 0 to 42 Å, which correspond to highly coiled and the fully extended, all trans conformations, are achieved many times during its dynamic trajectory. Though not shown here, this conclusion is further substantiated by plots of the PHB backbone torsion angles which evidence multiple transitions between their rotational states. The mean-square end-to-end distance calculated from the 10-mer dynamic trajectory was $\langle r^2\rangle_o = 403$ Å^2, leading to $C_r = 4.7$.

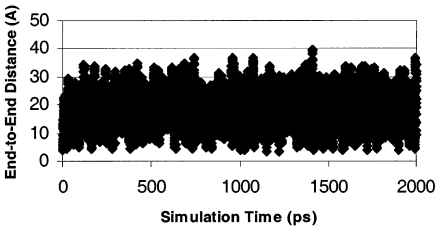

Figure 11. Plot of the end-to-end distance of the PHB 10-mer during its phantom chain molecular dynamics simulation.

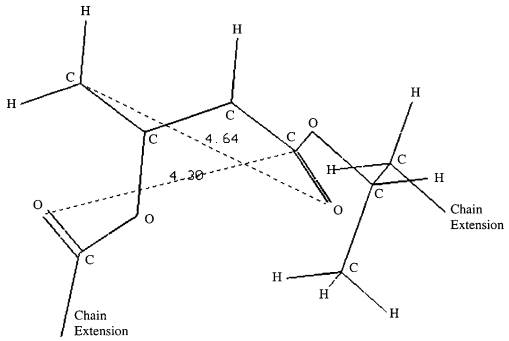

Figure 12. PHB segment in the $\tau = 0°$ (t), $\varphi = 280°$ (g^-), $\psi = 120°$ (g^+), and $\omega = 270°$ (g^-) conformations, where important nonbonded interactions were considered, that were ignored in the 5 and 4 Å cutoff distance simulations, and are illustrated.

(2)PHB 60- and 100-mers. Examination of the dynamic trajectories for the PHB 60- and 100-mers revealed behavior similar to the 10-mer trajectory, i.e., an adequate sampling of their complete conformational spaces. For the 60-mer $C_r = 7.4$ and 7.2 when the dynamic simulations were begun from randomly selected and the crystalline 2_1-helical conformations, respectively. For the PHB 100-mer a slightly larger $C_r = 8.0$ was obtained.

The probabilities or populations of backbone torsions evaluated from the dynamic trajectories of the PHB 60- and 100-mers were very similar to those of the 10-mer and the RIS models (see further discussion below). In addition, the population of PHB repeat units in the crystalline 2_1-helical conformation was found to be very low (<8%), and the simultaneous appearance of a few consecutive helical repeat units was almost nonexistent. When they did occur, they did not result in unusually large end-to-end distances.

The PHB 60-mer dynamic simulation was repeated with 4.0 and 6.0 Å cutoff distances for evaluation of the energetic interactions between nonbonded atoms and groups. Not surprisingly the larger cutoff distance resulted in the collapse of the 60-mer, with conformational transitions confined only to the chain ends. The shorter cutoff distance resulted in an adequate sampling of conformations and in the expansion of the average size of the 60-mer leading to a $C_r = 11.4$, which was also reflected in the comparison of backbone torsional populations between the trajectories conducted with 4.0 and 5.0 Å cutoffs. The 4 Å trajectory showed a slightly greater propensity for single and consecutive repeat units adopting the crystalline 2_1-helical conformation.

We prefer, however, to rely more heavily on the results for the simulations employing the 5 Å cutoff for the following reasons. In Figure 12, a PHB segment adopting the $\varphi = 280°$, $\psi = 120°$, and $\omega = 270°$ conformation is shown. The distances between the carbonyl oxygen and the methyl group of the same repeat unit and between the carbonyl oxygen and the

carbonyl carbon belonging to adjacent repeat units are between 4 and 5 Å. Both interactions in this PHB conformation are ignored/considered in the simulation employing a nonbonded interaction cutoff of 4/5 Å. To achieve a molecular dynamics simulation and conformational model representative of unperturbed PHB chains, interactions such as these must be considered. In addition, the average end-to-end distances obtained from the PHB 10-, 60-, and 100-mer molecular dynamics trajectories employing the 5.0 Å cutoff distance, i.e., $C_r = 4.7$, 7.2−7.4, and 8.0, appear to be converging with chain length, as they must for unperturbed chains that are unexpanded by long-range excluded volume interactions.[17]

The conformational characteristics of PHB, as simulated in the molecular dynamics trajectory of the 100-mer chain employing a 5.0 Å cutoff distance, can be summarized[27] in the form of the usual RIS statistical weight matrices, $\mathbf{U}_i$, for each backbone bond in the PHB repeat unit. This is achieved by tabulating the frequencies of occurrence or populations and positions of the neighboring pairs of backbone torsions (τ,φ), (φ,ψ), and (ψ,ω) (see Figures 1 and 9) observed during the course of the dynamics trajectory. When the statistical weight matrices evaluated from the PHB 100-mer dynamics trajectory, which are presented below, are used to directly calculate the average end-to-end distance of the 100-mer, $C_r = 4.2$ is obtained. This may be compared to the dimensions $C_r = 8.0$ yielded by averaging the end-to-end distances during the course of the 100-mer dynamics trajectory.

$$\mathbf{U}_{\varphi} = \begin{bmatrix} 0.59701 & 0.00597 & 0.39702 \\ 0.0 & 0.0 & 0.0 \\ 0.0 & 0.0 & 0.0 \end{bmatrix}$$

$$\mathbf{U}_{\varphi,\psi} = \begin{bmatrix} 0.14667 & 0.29090 & 0.07023 \\ 0.00171 & 0.00426 & 0.0 \\ 0.18848 & 0.16665 & 0.13110 \end{bmatrix}$$

$$\mathbf{U}_{\psi,\omega} = \begin{bmatrix} 0.06661 & 0.17399 & 0.09626 \\ 0.04700 & 0.26587 & 0.14894 \\ 0.01832 & 0.13784 & 0.04517 \end{bmatrix}$$

These dimensions differ by a factor of ca. 2, which is similar to the results obtained with the traditional and computer-generated RIS models, even though they yield similar bond conformational populations. This implies that independent, or intraresidue RIS models based on statistical weight matrices, whether generated during the molecular dynamics simulation of isolated PHB chains or obtained from conformational energy maps of pairwise dependent or complete intraresidue energies, under-estimate the unperturbed dimensions yielded by the molecular dynamics trajectories of isolated PHB chains and those observed experimentally in solution. This disparity must reflect the influence of interresidue interactions on the conformational characteristics of PHB, which are accounted for and neglected by the molecular dynamics simulation of isolated PHB chains and the independent, intraresidue RIS models, respectively.

(3) PHB 200-mer. The dynamic trajectory of the PHB 200-mer, on the other hand, did not suggest an adequate sampling of its conformational space. This is evident from the plots of the backbone torsion angles during the trajectory.

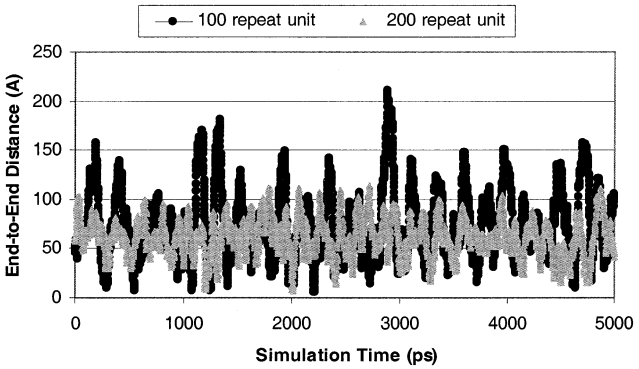

Figure 13. Plots of the end-to-end distances observed for the PHB 100-mer (black) and 200-mer (gray) during their phantom chain molecular dynamics simulation.

Though not shown, they reveal a considerable reduction in the number of conformational transitions when compared to the trajectories of the PHB 60- and 100-mers. Note in Figure 13, where the end-to-end distances observed during the dynamic trajectories of the PHB 100- and 200-mers are presented, that while the 100-mer repeatedly samples conformations spanning a substantial portion of the full range of its end-to-end distance values, the 200-mer does not. Instead the PHB 200-mer is restricted roughly to those conformations with end-to-end distance clustered around ∼50 Å. This behavior is seen clearly in the animations of the dynamic trajectories of the PHB 100- and 200-mers, where the 100-mer was observed to repeatedly coil and uncoil, while the 200-mer collapsed on itself at the beginning of the simulation and did not significantly change its overall size and shape during the remainder of the trajectory. The variation in the 200-mer end-to-end distances seen in Figure 13 were attributable solely to movement of the chain ends within the volume occupied by the collapsed chain, and not by large-scale conformational changes in the chain interior.

(d) Calculated Flexibility of PHB. Figure 9 presents a comparison of the PHB backbone conformational probability distributions calculated from the traditional RIS model and the phantom chain dynamics simulations for the PHB 10- and 60-mers. Each of the three potentially flexible PHB backbone bonds, characterized by the φ, ψ, and ω rotation angles (see Figure 1), do in fact exhibit considerable populations of at least two of their anticipated staggered states t, g^+, and g^-. The ψ torsion populates all three states with high probabilities, the ω torsion is primarily confined to $g^{\pm}$ states moderately displaced from ±120°, though the trans conformation is still accessible, and the ø torsion is limited to substantially populated g^- and t states separated by a low barrier, which suggests almost unlimited access to $\varphi = 250-360°$ rotations. There is certainly very little in these results to suggest that the PHB chain would be expected to highly favor specific repeat unit conformations, with limited transitions between them, and thus evidence significant persistence of local conformations.

Though both the RIS models and phantom chain dynamics simulations of isolated PHB chains strongly point to flexible, randomly coiling conformational behavior, the dimensions yielded by the molecular dynamics trajectories are over twice as large as those obtained from the RIS models for PHB.

The torsional population distributions in Figure 9 indicate a greater disparity in the $\omega = g^{\pm}$ populations,

and the more extended $\varphi = t$ conformation is favored over the $\varphi = g^-$ conformation when comparing the molecular dynamics simulation and RIS torsional populations. Both of these conformational differences would be expected to lead to larger conformationally averaged dimensions for PHB when simulated as phantom chains by molecular dynamics.

2. Comparison of Calculated and Observed Dimensions. (a) Dimensions in Solution. The unperturbed dimensions measured[12−15] for PHB in dilute solution lead to $C_r \sim 8$, whether measured in a Θ solvent or extrapolated to unperturbed conditions from measurements performed in good solvents, where the PHB chain is highly expanded ($\alpha \geq 2$, where $\alpha^2 = \langle r^2\rangle/\langle r^2\rangle_o$). Dimensions calculated from the traditional and computer-generated RIS model yield $C_r \sim 3-4$, which underestimate the observed dimensions even when the traditional RIS model is modified to account for intrachain interactions dependent upon more than nearest-neighbor pairs of backbone rotations. In addition, the dimensions calculated for PHB chains from the RIS models are independent of their stereosequence in accordance with observations by Einaga et al.[14] in solution.

Molecular dynamics trajectories of isolated PHB chains, which account for all interactions between atoms separated by distances ≤5 Å, result in dimensions ($C_r \sim 8$) in accordance with those measured in solution. Examination of these trajectories reveals a low occurrence of PHB repeat units simultaneously adopting helical conformations and an almost vanishing population of consecutive, neighboring PHB repeat units assuming helical conformations.

(b) Dimensions in the Bulk. The SANS observation[16] of d-PHB in the quenched-melt lead to locally persistent chains, which appear Gaussian in their global behavior, and yield dimensions, $C_r \sim 40$, five times larger than those observed for unperturbed PHB chains in dilute solutions. These large dimensions may only be obtained from the RIS models if more than 15% of the central residues in PHB chains are arbitrarily restricted to the helical conformation, if 90% helical, random-coil repeat units are placed randomly, or if the PHB chain is required to adopt 50% helical repeat units arranged in blocks. For example, $C_r \sim 40$ is calculated for a PHB chain of 1000 repeat units when blocks of 50 helical and 50 randomly coiling repeat units are placed in regular alternation. It should be remembered that the molecular dynamics simulations of PHB showed no significant evidence for helical conformations, and much less for helical clusters.

Conclusions

RIS models, both traditional and computer-generated, and molecular dynamics simulations of isolated PHB chains result in unperturbed conformations and dimensions which are independent of their stereosequence and are characteristic of a randomly coiling polymer chain. No evidence is observed for the tendency of PHB chains to locally adopt helical conformations, such as the 2_1-helix assumed by PHB when it crystallizes (see Figure 2). These results are consistent with the dilute solution behavior reported[12−15] for PHB but are at odds with the locally stiff description of PHB chains and the resultant large dimensions obtained by SANS observations[16] of d-PHB in a melt-quenched blend with protonated a-PHB.

References and Notes

(1) Lemoigne, M. *Ann. Inst. Pasteur* **1927**, *41*, 146.
(2) Doudoroff, M.; Stanier, R. Y. *Nature (London)* **1959**, *183*, 1440.
(3) Wilkinson, J. F. *J. Gen. Microbiol.* **1963**, *32*, 171.
(4) Macrae, R. M.; Wilkinson, J. F. *J. Gen. Microbiol.* **1958**, *19*, 210.
(5) Williamson, D. H.; Wilkinson, J. F. *J. Gen. Micrbiol.* **1958**, *19*, 198.
(6) Hocking, P. J.; Marchessault, R. H. In *Chemistry and Technology of Biodegradable Polymers*; Griffen, G. J. L, Ed.; Blackie Academic and Professional: Glasgow, Scotland, 1994, Chapter 4.
(7) King, P. P. *J. Chem. Technol. Biotechnol.* **1982**, *32*, 2.
(8) Cornibert, J.; Marchessault, R. H. *J. Mol. Biol.* **1972**, *71*, 735.
(9) Yokouchi, M.; Chatani, H.; Tadokoro, K.; Teranishi, K.; Tani, H. *Polymer* **1973**, *14*, 267.
(10) Marchessault, R. H.; Okamura, K.; Su, C. J. *Macromolecules* **1970**, *3*, 735.
(11) Cornibert, J.; Marchessault, R. H.; Benoit, H.; Weill, G. *Macromolecules* **1970**, *3*, 741.
(12) Aikita, S.; Einaga, Y.; Miyaki, Y.; Fujita, H. *Macromolecules* **1976**, *9*, 774.
(13) Miyaki, Y.; Einaga, Y.; Hirosye, T.; Fujita, H. *Macromolecules* **1977**, *10*, 1356.
(14) Kurata, M.; Tsunashima, Y. In *Polymer Handbook*, 3rd ed.; Brandup, J., Immergut, E. H., Eds.; Wiley: New York, 1989; Chapter VII.
(15) Huglin, M. B.; Radwan, M. A. *Polymer* **1991**, *32*, 1293.
(16) Beaucage, G.; Rane, S.; Sukumaran, S.; Satkowski, M. M.; Schectman, L. A.; Doi, Y. *Macromolecules* **1997**, *30*, 4158.
(17) Flory, P. J. *Statistical Mechanics of Chain Molecules*; Wiley: New York, 1969.
(18) Brant, D. A.; Tonelli, A. E.; Flory, P. J. *Macromolecules* **1969**, *2*, 228.
(19) Biosym/MSI *Polymer 3.0.0 User Guide*, Part 1; 1995; Chapter 3.
(20) Hedenqvist, M. S.; Bharadwaj, R.; Boyd, R. H. *Macromolecules* **1998**, *31*, 1556.
(21) The term "phantom chain" usually[22] implies a polymer chain whose segments are not prohibited from self-intersecting to simultaneously occupy the same volume and are therefore free from excluded volume effects. In the "phantom chain" modeling employed by Hedenqvist et al.[20] and us, the energetic interactions between atoms within a through-space cutoff distance are considered, independent of their separation along the chain contour. Thus, as segments separated along the chain contour approach each other closely through space, their energetic interactions will prevent them from completely overlapping, and so use of the term "phantom chain" is in this sense not entirely traditional.
(22) James, H. M.; Guth, E. *J. Chem. Phys.* **1947**, *15*, 669.
(23) Nosé, S. *J. Chem. Phys.* **1984**, *81*, 511.
(24) Nosé, S. *Mol. Phys.* **1984**, *52*, 255.
(25) Hoover, W. G. *Phys. Rev. A*, **1985**, *31*, 1695.
(26) Biosym/MSI *Discover 2.9.7/95.0/3.0.0 User Guide*, Part 1; 1995; Chapter 3.
(27) Mattice, W. L.; Dodge, R.; Zuniga, I.,; Bahar, I. *Comput. Polym. Sci.* **1991**, *1*, 35.

MA0200827